7. Solve Problem 2 of Chapter 9 if the component is to operate at −40°C (−40°F). Discuss the significance of your assumptions and the accuracy of your results.

8. If a wide plate has a through-thickness edge crack of 3 mm and the applied $R = 0$ stress range causes an initial $\Delta K = 18$ MPa$\sqrt{m}$, how many constant amplitude cycles of this stress range can be applied before fracture at room temperature and −160°C for the steel in Fig. 11.12*a*? Comment on your calculation procedures and results.

9. Discuss the ideas of Problem 13 in Chapter 9 for a temperature of −40°C (−40°F) and a liquid nitrogen temperature of −195°C (78 K).

10. Determine the effect of temperature on K_f in Fig. 11.17. Consider all four temperatures and $A = \infty$, 2.0, and 0.25.

11. Solve Problems 19*a* and 19*b* in Chapter 7, assuming that $\Delta\varepsilon/2 = 0.01$ and $P_a = 100$ kN and the component is annealed 304 stainless steel operating at 7 Hz and 500°C. Comment on the accuracy of your predictions.

12. A CrMoV steel tested at 550°C is subjected to fatigue cycles similar to that shown in Fig. 11.20*b*. Based on existing experimental data, the following relationships were determined: $\Delta\varepsilon_{cc} = 0.14(N_{cc})^{-0.45}$, $\Delta\varepsilon_{pp} = 0.48\,(N_{pp})^{-0.52}$, and $\Delta\varepsilon_{pc} = 0.27(N_{pc})^{-0.49}$. From the hysteresis loop, the following information was obtained: $\Delta\varepsilon_{cc} = 0.0085$, $\Delta\varepsilon_{pp} = 0.0123$, and $\Delta\varepsilon_{pc} = 0.0012$.
(*a*) Draw the strain-range partitioning relationships for this alloy,
(*b*) Determine the total number of cycles for the above strains that will cause failure.

13. Solve Problem 12*a–c* of Chapter 6, assuming that the plate is to operate at 93°C (200°F) where $K_{Ic} = 44$ MPa$\sqrt{m}$. Assume that the Paris relationship for long crack behavior at $R = 0$ and 93°C is $da/dN = 8.5 \times 10^{-11}(\Delta K)^{3.85}$ where da/dN is in m/cycle and ΔK is in MPa$\sqrt{m}$. Also, do you expect creep to be of significance in this problem? Explain your reasoning.

CHAPTER 12

FATIGUE OF WELDMENTS

Parts and structures are often welded together in some fashion, usually due to cost and weight effectiveness. Steels, followed by aluminum alloys, are the most frequently welded metals, while some metals cannot be effectively welded. Weldments present difficulties because of macro and micro discontinuities, residual stresses, and posssible misalignment, all of which may vary between nominally equal parts. Weldments are frequently the prime location for fatigue failures. Welding itself is a complex procedure that can result in a wide range of fatigue resistance. The quality of workmanship and the design determine the fatigue resistance of weldments. A carefully designed and processed weldment can develop the same fatigue strength as a part forged and machined from one piece, and at far less cost. An aircraft part that incorporates a nose wheel spindle and a landing gear piston in one piece of high-strength steel may serve as an example of a carefully designed weldment having good fatigue resistance. The parts are rough machined from a material like 4340 steel, welded together, finish machined, heated in a controlled atmosphere, quenched in oil, tempered to achieve the desired hardness, and shot-peened. By contrast, an attachment to a machine using an untreated fillet weld can substantially reduce the fatigue resistance of the machine.

We consider different weldments from a fatigue design viewpoint by indicating the different macro and micro discontinuities that can exist, typical fatigue behavior, and methods for improving weldment fatigue resistance. We then briefly discuss the four fatigue design procedures (*S–N*, *ε–N*, *da/dN–ΔK*, and the two-stage method) outlined in previous chapters for application to weldments, along with current weldment design codes.

12.1 WELDMENT NOMENCLATURE AND DISCONTINUITIES

Several typical weldments are shown schematically in Fig. 12.1 with accompanying fatigue strengths for structural steel at 2×10^6 cycles with $R = 0$ [1]. These are rather simplified welded joints, but they do represent many real

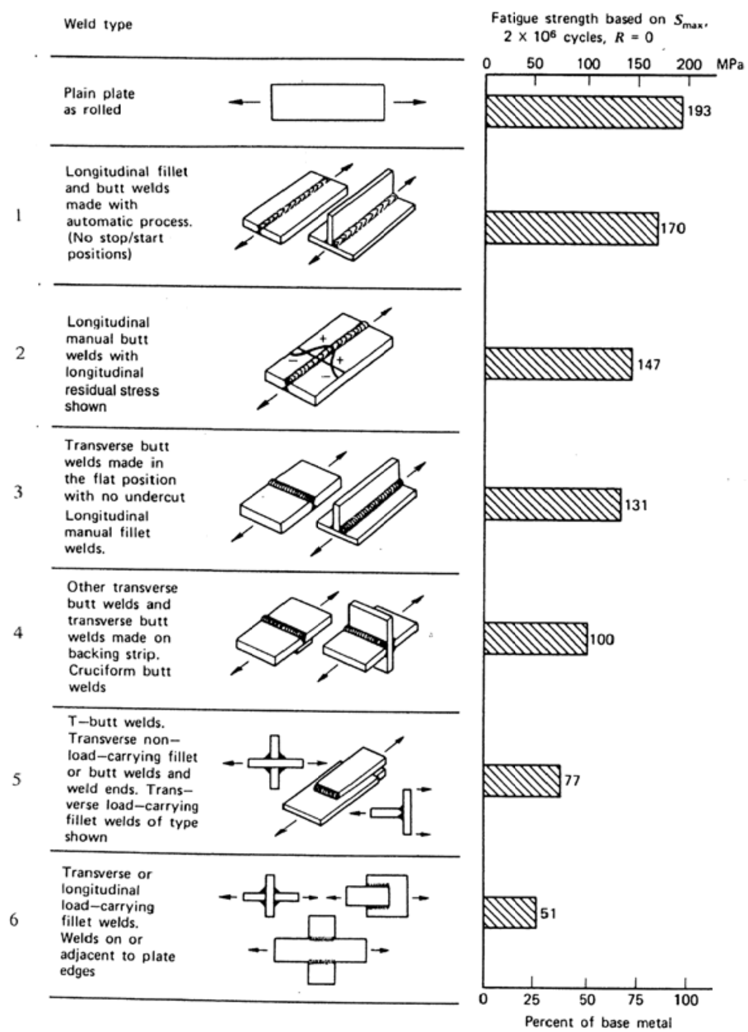

Figure 12.1 Weld type and fatigue strengths for structural steel [1].

parts and structures. In general there are butt, fillet, and spot welds with many different weldment shapes and configurations. Both transverse butt and longitudinal butt welds are common. Fillet welds, however, are more common and, as shown in Fig. 12.1, may be load carrying, as in the left of row 6, or non-load carrying, as in the left of row 5. The limited fatigue strengths given in Fig. 12.1 range from about 25 to 90 percent of the unnotched as-rolled base plate fatigue strength and provide a reasonable guide for actual variation in weldment fatigue strengths, depending on the weldment. The range from 25 to 90 percent indicates a significant difference in weldment fatigue strengths.

Because of nonuniform temperature gradients and thermal expansion and contraction that cause local elastic/plastic deformations during the welding and cooling process, biaxial or triaxial residual stresses are formed in all welds. The residual stress profiles and their magnitudes are difficult to quantify. Figure 8.14*a* and Fig. 12.1, row 2, show a typical longitudinal residual stress distribution at a transverse section. The residual stresses are tensile in the weld region, which must be balanced by compressive residual stresses away from the weld. The tensile stresses may reach values equal to the yield strength and can contribute to the lower fatigue resistance of some weldments. Residual stresses in weldments are considered in more detail in Section 12.3.

A photograph of a polished and etched longitudinal section of a cruciform fillet weldment obtained by Albrecht [2] is shown in Fig. 12.2. The toe and root of the weldment are indicated, along with three basic weldment regions:

1. Parent or base metal (BM)
2. Deposited weld metal (WM)
3. Heat affected zone (HAZ)

In addition, a fourth region, a fusion zone, exists between the deposited weld metal and the heat affected zone. These four regions can have different microstructures, residual stresses, discontinuities, and monotonic strength, ductility, and fracture toughness properties. The heat-affected zone is the base metal, which is subjected to high-temperature gradients during welding. The higher temperature adjacent to the fusion line causes recrystallization, while other regions of the heat-affected zone may not completely recrystallize. Thus, mechanical properties and metallurgical structures may vary across the width of the heat-affected zone and may be similar to, or different from, the base metal. For welded aluminum alloys, the heat-affected zone thermally softens to a condition similar to an annealed base metal condition.

Figure 12.3 shows transverse sections of full and partial penetration butt and fillet weldments. Common locations for cracks to nucleate and/or grow are shown for each weldment. Stress concentrations, which occur at the toe of butt and fillet welds, are common locations for fatigue cracks. The toe is also at the surface, where bending stresses are the largest. K_t at the toe depends on the geometry of the weld, as defined in Fig. 12.3*b*, and is usually larger in

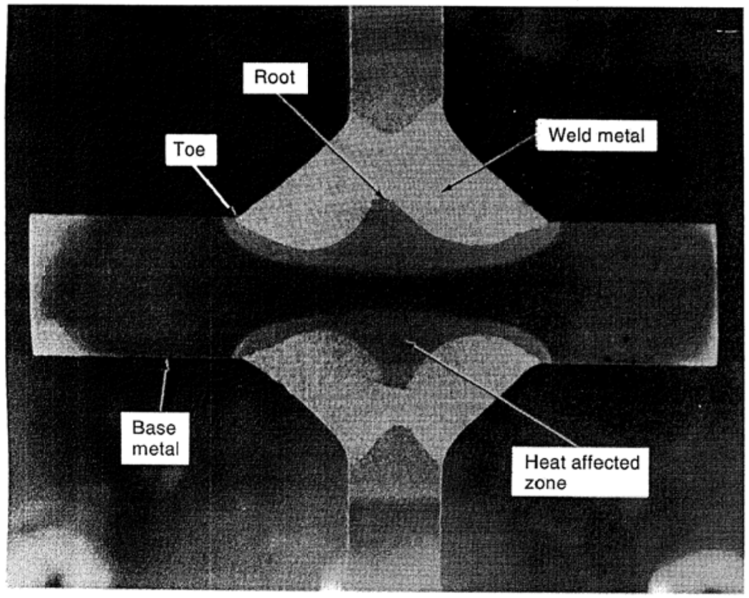

Figure 12.2 Polished and etched longitudinal section through a non-load-carrying cruciform weldment [2] (reprinted by permission of the American Society for Testing and Materials).

fillet welds than in butt welds. Values of K_t have ranged from essentially 1 for butt welds with the reinforcement removed to 3 to 5 for sharp geometrical changes in fillet welds. The word "reinforcement" is a misnomer since it implies a positive effect. Actually, the "reinforcement" acts as a stress concentration, is detrimental in fatigue, and should be called "overfill" or perhaps "excess" weld metal. Fatigue cracks also grow at the weld root, as shown in Fig. 12.3 for fillet welds and partial penetration butt welds.

There are always macro and/or micro discontinuities in weldments that provide sites for cracks to nucleate. Some of these discontinuities may actually be planar, as in the case of cracks, and hence crack nucleation fatigue life may be zero or small in this case. Fatigue life in weldments is then considered to involve only fatigue crack growth life [3,4]. When crack-like discontinuities do not exist, weldment fatigue life may be considered to consist of fatigue crack nucleation and fatigue crack growth of small cracks leading to the growth of large cracks [5,6]. Whichever philosophy or situation is most relevant, significant agreement exists that fatigue crack growth plays a dominant role in fatigue of weldments. An important key aspect of weldments then is the reduction of macro and micro discontinuities which will enhance fatigue crack nucleation life and thus enhance total fatigue life.

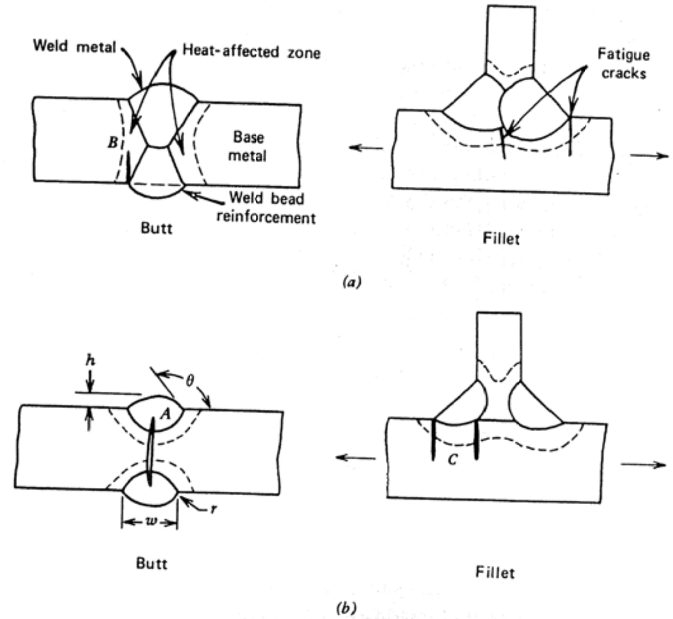

Figure 12.3 Weldment nomenclature and fatigue crack nucleation and/or growth sites. (*a*) Full penetration welds. (*b*) Partial penetration welds.

Weldment discontinuities can be classified as planar, volumetric, or geometric as follows:

Planar discontinuities: solidification cracks, shrinkage cracks, hydrogen-induced cracks, lamellar tears, lack of fusion, partial penetration, or sharp oxide inclusions.

Volumetric discontinuities: porosity or slag inclusions.

Geometric discontinuities: stop/start/terminations/intermittent locations, surface ripples, reinforcement, toe radius, toe undercutting, overlaps, section changes, misalignment, stray arc strikes, or spatter.

Solidification cracks may occur in the deposited weld metal and are caused by excessive restraint on adjacent material as the metal cools from liquid to solid. Shrinkage cracks are due to cooling temperature gradients and can occur in metal that has not been melted. Hydrogen can be introduced during welding from surface water, oil, grease, or paint and welding flux and can cause cracking in high cooling rate regions containing higher carbon contents.

Lamellar tears can develop during welding at prior elongated inclusions formed during rolling operations. Porosity is caused primarily by trapped gases during solidification, and slag inclusions form from the electrode coating. Many of these discontinuities occur at the surface or intersect the surface, and many are also subsurface. The planar discontinuities are crack-like and are thus considered to be cracks. The shapes of porosity and slag inclusions are often somewhat rounded, and hence may not represent crack-like discontinuities and are thus considered less harmful. Geometric discontinuities more closely resemble macro stress concentrations.

Figure 12.3 indicates that fatigue cracks may nucleate and/or grow in the weld metal (A) or in the heat-affected zone (B) or through the heat-affected zone and the base metal (C). Thus, we should have information about fatigue behavior in all three zones.

12.2 CONSTANT AMPLITUDE FATIGUE BEHAVIOR OF WELDMENTS

12.2.1 Stress–Life (S–N) Behavior

Most steels used in weldments have yield strengths below 700 MPa (100 ksi). Even with strengths above this value, much information indicates that for a given transverse butt or fillet weldment, as-welded constant amplitude fatigue strengths at 10^6 cycles or more are rather independent of material ultimate tensile strength. This was shown by Reemsnyder [7] for transverse butt weldments using a number of steels in different conditions with tensile strengths varying from 400 to 1030 MPa (58 to 148 ksi). The geometric notch severity of the weldment, residual stresses which may or may not relax, other discontinuities, loss of heat treatment, and cyclic softening or hardening are the causes of this behavior. As we see later, however, methods do exist to improve weldment fatigue resistance.

Geometrical stress concentrations have a significant effect on weldment fatigue resistance. The influence of the reinforcement angle for transverse butt welds is shown in Fig. 12.4 [1]. Here we see that a factor of almost 2 exists for the fatigue strength at 2×10^6 cycles as the reinforcement angle varies from 100° to 150°. Reemsnyder [7] showed that decreasing the height h of the transverse butt weld reinforcement continually improved the fatigue strengths of 785 MPa (114 ksi) ultimate tensile strength steel, as shown in Fig. 12.5. Fatigue notch factors, K_f, at 2×10^6 cycles were 4.5, 2.5, 1.5, and essentially 1.0 as the height was decreased from 3.8 mm to complete reinforcement removal. Thus, S_f for the transverse butt weldment with reinforcement removed is very similar to that for the base metal. However, care must be taken during grinding of the reinforcement so as not to introduce excess grinding notches that could be more detrimental than the reinforcement. Sanders and Lawrence [8] also showed significant improvement in fatigue strength in alumi-

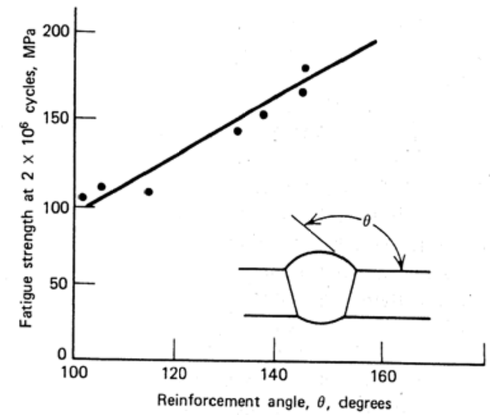

Figure 12.4 Influence of reinforcement shape on fatigue strength of transverse butt welds [1].

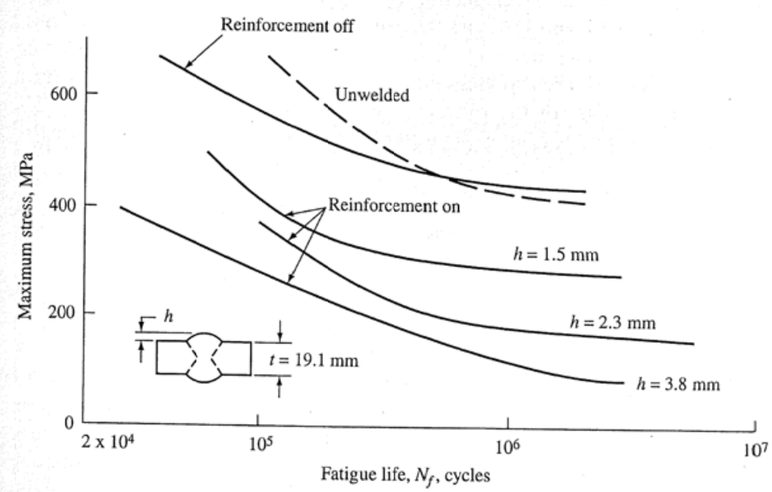

Figure 12.5 S–N curves for transverse butt welds, Q&T carbon steel, S_u = 785 MPa (114 ksi), R = 0 [7] (reprinted by permission of the American Society for Testing and Materials).

num alloy transverse butt welds when the reinforcement was removed. Thus, it should be clear that reducing stress concentrations in weldments is a major factor in improving fatigue resistance.

Mean stress influence on fatigue resistance of weldments is similar to that of other severely notched components. A constant-life diagram with S_a versus S_m for carbon steel butt welds is shown in Fig. 12.6 [7]. The resemblance of Fig. 12.6 to the Haigh diagram for notched parts (e.g., Fig. 7.10) is quite strong. Figure 7.10 for notches indicates appreciable influence from compressive mean stress and significantly smaller influence from tensile mean stress. Tensile mean stresses in weldments do not have an appreciable effect on the allowable alternating stress, and therefore it has become common practice to disregard tensile S_m in weldment fatigue design codes. This small tensile S_m effect is due to local plasticity at the weld toe or root caused by superposition of applied stresses with high tensile residual stresses remaining after the welding process. Compressive mean stresses are found to enhance fatigue resistance, as shown in Fig. 12.6. However, they also are commonly neglected in most weldment fatigue design codes.

12.2.2 Strain–Life (ε–N) Behavior

Cyclic stress–strain data and strain–life (ε–N) fatigue data for the three weldment regions have been determined by Higashida et al. [9] for A36 steel, A514 steel, and 5083 aluminum alloy. Cyclic softening was predominant in the A36 steel WM and HAZ metal. Even greater cyclic softening occurred in the A514 WM, BM, and HAZ metal. For the aluminum alloy, cyclic hardening occurred in the WM and BM. Strain–life (ε–N) curves for the A36 steel weldment materials are shown in Fig. 12.7 and monotonic, cyclic stress–strain, and ε–N properties for the different materials are given in Table 12.1. The general trend found for the ε–N curves for the three weldment regions is that

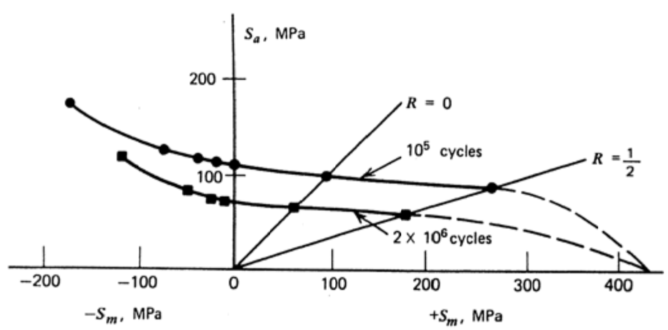

Figure 12.6 Constant-life diagram for carbon steel butt welds [7] (reprinted by permission of the American Society for Testing and Materials).

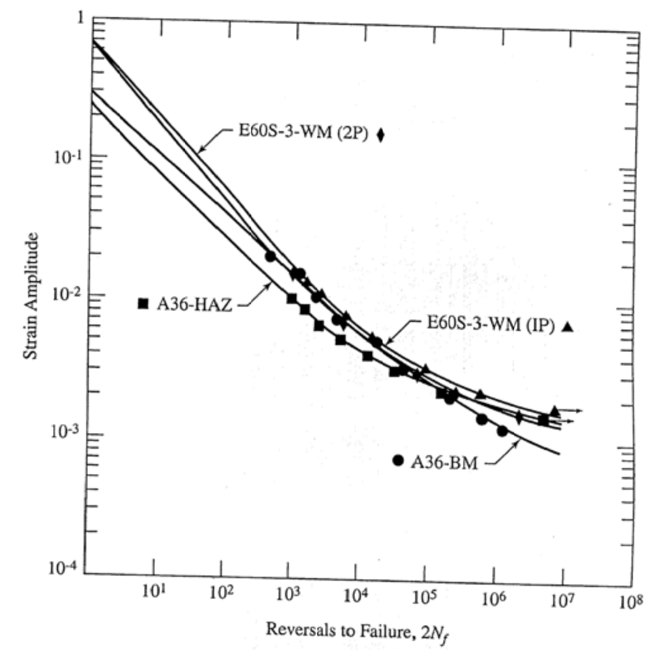

Figure 12.7 Strain-controlled fatigue behavior of A36 steel weldment materials [9] (reprinted with permission of the American Welding Society).

the softer materials have better fatigue resistance at short lives, while the harder materials have better fatigue resistance at long lives. This finding agrees with the ε–N data described in Fig. 5.13.

12.2.3 Crack Growth (da/dN–ΔK) Behavior

Maddox [10] obtained region II fatigue crack growth data for weld metals with S_y ranging from 386 MPa (56 ksi) to 636 MPa (92 ksi), a simulated heat-affected zone, and C-Mn base metal, as shown in Fig. 12.8. Eleven different conditions are superimposed in this figure. The scatter band for all stress intensity factor ranges varied from 2 to 1 and from 3 to 1 for crack growth rates between 10^{-8} and 3×10^{-6} m/cycle (4×10^{-7} and 1.2×10^{-4} in./cycle), respectively. This small scatter band implies that region II fatigue crack growth behavior is similar in sound weldments. James [11] also indicated that this same behavior occurs in pressure vessel steel weldments. Fatigue crack growth in weldments is also somewhat independent of tensile mean stress in region II. The small scatter in da/dN–ΔK behavior and the small influence from S_m for

TABLE 12.1 Monotonic and Cyclic Strain Properties of Some Weld Materials: SI Units [9]

	S_u, (MPa)	S_y/S_y', (MPa/MPa)	K/K', (MPa/MPa)	n/n'	$\varepsilon_f/\varepsilon_f'$	σ_f/σ_f', (MPa/MPa)	b	c
A36 base metal	414	225/230	780/1100	/0.25	1.19/0.27	950/1015	−0.132	−0.45
A36 HAZ	667	530/400	980/1490	0.102/0.215	0.74/0.22	920/720	−0.070	−0.49
E60S weld metal	710	580/385	990/1010	0.098/0.155	0.59/0.61	990/900	−0.075	−0.55
E60 weld metal	580	410/365	850/1235	0.130/0.197	0.93/0.60	1015/1030	−0.090	−0.57
A514 base metal	938	890/600	1190/1090	0.060/0.091	0.99/0.97	1490/1305	−0.080	−0.70
A514 HAZ	1408	1180/940	2110/1765	0.092/0.103	0.75/0.78	2250/2000	−0.087	−0.71
E110S weld metal	1035	835/650	1560/2020	0.092/0.177	0.86/0.85	2210/1890	−0.115	−0.73
E110 weld metal	910	760/600	1290/1670	0.085/0.166	0.90/0.59	1660/1410	−0.079	−0.59
5083-0 aluminum base metal	294	130/290	300/580	0.129/0.114	0.36/0.40	415/710	−0.122	−0.69
5183 aluminum weld metal	299	140/270	310/510	0.133/0.072	0.40/0.58	420/640	−0.107	−0.89

Reprinted with permission of the American Society for Testing and Materials.

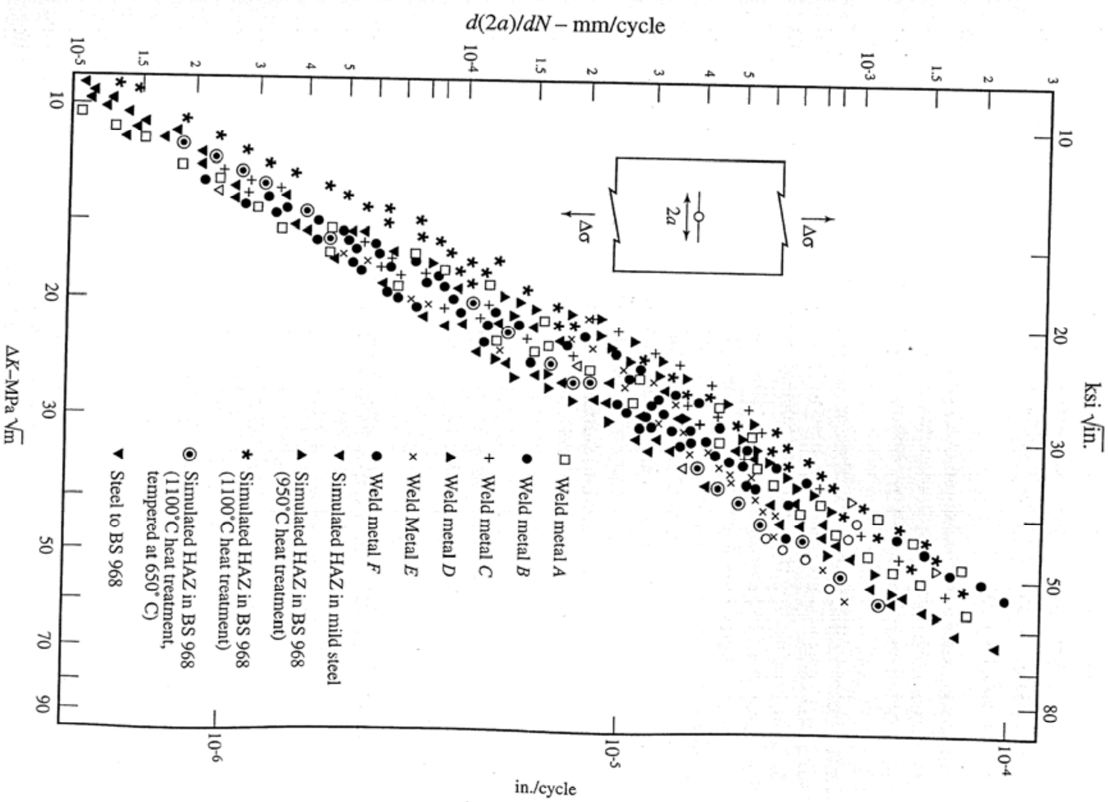

Figure 12.8 Fatigue crack growth data for structural C–Mn steel weld metals, HAZ, and base metals [10] (reprinted with permission of the American Welding Society).

a variety of steel weld metals and base metals have been important influences in formulating steel weldment design codes.

12.2.4 Spot Welds

Spot welds usually fail in fatigue through the sheet at long lives and through the nugget at short lives or in monotonic loading. Failure through the nugget occurs by nugget shear or nugget pullout from the heat-affected zone. Fatigue failure through the sheet involves initial cracking at the nugget edge in the heat-affected zone, with cracks then growing through the base metal. Fatigue strengths can be substantially less than those for the base metal alone, and this can be significantly attributed to high multiaxial stress concentrations. Typical spot weld lap joint fatigue strengths can range from 15 to 30 percent of the base metal fatigue strength with single or multiple rows of spots. The number of spot weld rows and their alignment can alter fatigue resistance. The ultimate tensile strength of the base metal, as with other weldments, does not have a major influence on fatigue of spot welds [6]. Fatigue strength of spot welds decreases with greater sheet thickness due to the usual thickness effects and additional secondary bending stresses from out-of-plane loading of lap joints. S–N, ε–N, da/dN–ΔK, and the two-stage methods have been used for spot weld fatigue design. Modifications of stress intensity factors for spot welds have been made to incorporate the stress ratio, weldment geometry, and the presence of mixed-mode fatigue crack growth. See [12] for additional information on spot weld design.

12.3 IMPROVING WELDMENT FATIGUE RESISTANCE

There are essentially four basic ways of improving weldment fatigue resistance:

1. Improve the actual welding procedure.
2. Alter the material microstructure.
3. Reduce geometrical discontinuities.
4. Induce surface compressive residual stresses.

These four methods actually overlap, since improving the welding procedure can improve the microstructure, reduce the stress concentrations, and alter residual stresses. We mentioned earlier that substantial differences in weld metal ultimate tensile strengths have not provided accompanying large differences in the fatigue resistance of as-welded joints. Thus, in improving weldment fatigue resistance, the major emphasis is on reducing geometrical discontinuities and the use of compressive residual stresses. Many of these improvements involve post weld treatments that add cost to the product and, therefore, perhaps have not received enough use during manufacture. In many instances,

careful consideration of applying improvement methods only to critical areas may significantly justify the expense. Post weld improvement methods have also been used for modifications, repairs, and when higher applied loads are planned.

Reducing Geometrical Discontinuities Removing the reinforcement from butt welds is the most obvious improvement. Careful grinding can be the quickest way to accomplish this. Fillet weld toe profiles can be improved by careful grinding, but since fatigue cracks often grow from either the toe or the root, this may sometimes shift the failure location without increasing fatigue resistance, particularly with only partial penetration welds. Tungsten arc inert gas (TIG) dressing of welds causes local remelt and can improve the weld profile by rounding the fillet toe and removing trapped inclusions, porosity, surface cracks, and undercuts at the weld toe. Large changes in stiffness at welds should be avoided. Choose butt welds rather than lap joints if possible. Start/stop positions, weld ends, and even arc strikes are common locations for fatigue cracks to nucleate and grow. Careful local grinding can improve the fatigue resistance of these regions. All of the above grinding and dressing operations must be done with care. Otherwise, stress concentrations greater than that resulting from the original welding can occur, lowering fatigue resistance. Intersecting welds and excess surface ripples should be avoided. Partial penetration essentially provides a crack-like planar discontinuity that should be avoided. Thus, good detail design can appreciably increase weldment fatigue resistance. Additional beneficial design details can be found in references and design codes discussed in Section 12.4.

Altering Residual Stresses Common methods used to induce desirable surface compressive residual stresses in weldments include shot- and hammer-peening, surface rolling, spot heating, and tensile or proof overloading. Thermal stress relieving has been used to reduce tensile residual stresses. Each of these operations can provide a substantial increase in fatigue resistance or can be ineffective. This inconsistency is due to relaxation of the residual stresses in the lower-strength weldment materials caused by repeated loading. For example, a single high compressive load can remove much of the desirable compressive residual stress. Since residual stresses can be as high as the yield strength, better improvement from compressive residual stresses can be expected with the higher-strength weldments.

It appears that mild usage of the above methods for inducing compressive residual stresses will not substantially improve fatigue resistance. Reemsnyder [7] indicated that shot-peening of non-load-carrying fillet welded carbon steel and butt welded Q&T alloy steel produced 20 to 40 percent increases in S_f. However, peening to half of the arc height for the above welds resulted in only 7 percent improvement. For significant and repeatable improvements, shot-peening must be closely controlled. Hammer-peening requires even greater quality assurance control in order to ensure repeatable and adequate

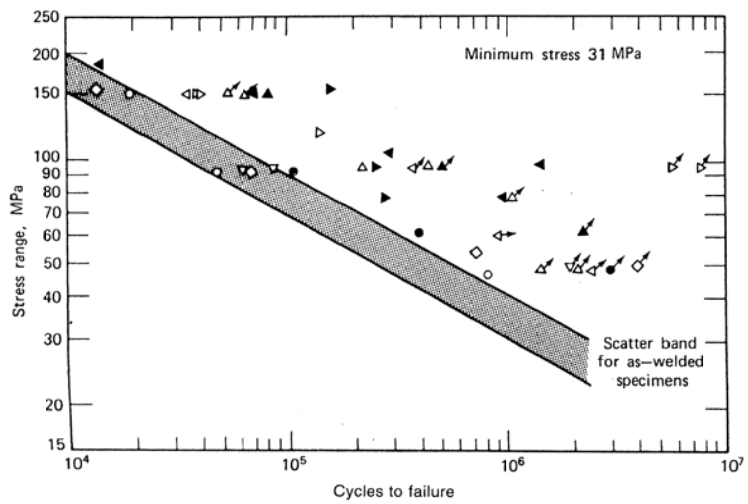

Figure 12.9 The effect of potential life improvement methods of non-load-carrying Al–Zn–Mg (7005) fillet welds [13] (reprinted by permission of the American Society for Testing and Materials) (○) shot-peened, (▽) ground, (●) ground and shot-peened, (△) hammer-peened, (▲) ground and hammer-peened, (◁) one preload, (▷) ten preloads, (◀) one overload every 1000 cycles, (▶) 10 overloads every 1000 cycles, (◇) grit blast and paint, (↗) unfailed or failure remote from the transverse weld toe.

compressive residual stress fields and depths. The fatigue resistance of spot welds can be increased by static overloading or by applying compression (coining) directly to the spot.

Weber [13] determined the effect of various methods of inducing compressive residual stresses in 7005 aluminum alloy weldments. These results are shown in Fig. 12.9. Light shot-peening or grit blasting did not improve fatigue resistance, but a more severe hammer-peening was effective. Multiple tensile overloads were better than single overloads.

12.4 WELDMENT FATIGUE LIFE ESTIMATION

12.4.1 General Weldment Fatigue Life Models

General methods for estimating fatigue life are given in previous chapters. One method involves using S–N behavior and the Haigh or modified Goodman diagrams for mean stress. Another method uses ε–N behavior with a notch strain analysis model and Morrow or SWT models for mean stress. A third method involves da/dN–ΔK integration with Forman, Walker, or other models

for mean stress. The two-stage method using both ε–N and da/dN–ΔK to include both fatigue crack nucleation and fatigue crack growth can also be used. The S–N approach developed from fatigue tests of weldments is historically, and currently, the most common weldment fatigue design method. The aforementioned four methods are applicable to both constant and variable amplitude loading of weldments. The later also involves cycle counting and cumulative damage in which rainflow counting and the Palmgren-Miner linear damage rule are most commonly used. These same procedures can be, and have been, used in weldment fatigue life estimates. However, additional complications exist, involving the following:

1. Determining realistic values of the fatigue notch factor, K_f.
2. Incorporating the local multiaxial stress state caused by the weldment notch geometry even under uniaxial loading.
3. Determining fatigue strength, S_f, strain–life fatigue properties, σ_f', ε_f', c, and b (Eq. 5.14), da/dN–ΔK properties, A and n (Eq. 6.19), or equivalent expressions, and fracture toughness for weldment materials.
4. Including welding and deliberate multiaxial residual stresses when relaxation of residual stresses may be present.
5. Making basic assumptions about what size discontinuities, including cracks, may exist in weldments following welding.
6. Determining realistic stress intensity factors for small cracks in weldments.

Item 1 could be handled by assuming a value of K_f. However, K_f can vary from about 1 up to about 5 for $R = -1$ and 10^6 or 10^7 cycles. Thus, some information on welding quality for each product would be needed.

Item 2 could be handled by using an equivalent nominal stress or an equivalent stress intensity factor. The multiaxial stress state resulting from weld geometry is accounted for in the S–N curve generated for a specific weldment geometry and loading.

The fatigue properties specified in item 3 are often similar to base metal values, which can be used as a starting point in the analysis. If actual weldment fatigue properties are known, they of course should be used.

Residual stress relaxation (item 4) in low-strength weldments is quite common. For higher-strength weldment materials, however, stress relaxation is much less. Hence, surface compressive residual stresses can be one of the best ways to improve the fatigue resistance of high-strength weldment materials.

Item 5 is quite controversial, but since crack-like discontinuities may exist in weldments, calculations have been made based only on fatigue crack growth from an initially small crack-like discontinuity. Successful estimates of fatigue life have also been made using S–N or ε–N data. The two-stage method is also relevant to weldments.

A primary problem of item 6 is deciding what stress to use in the vicinity of a weld notch that contains a steep stress gradient. A simple approach is to use the product of nominal stress and K_t while the crack tip is near the notch discontinuity. However, K_t values in weldments are difficult to obtain and involve significant variability. Stress intensity factor solutions for cracks emanating from notches, although not extensive for either applied or residual stresses, are given in stress intensity factor handbooks [14,15] and in welding design codes and handbooks. The surface elliptical crack is of greatest importance in weldments.

12.4.2 Weldment Fatigue Design Codes and Standards

The above complications have been somewhat overcome with many years of national and international cumulative experience involving many industries and professional societies devoted to formulating and updating weldment fatigue design codes and standards. Examples of these fatigue design codes or standards are given in [16–24]. These codes or standards provide significant quantitative information on weldment fatigue design and inspection and are based primarily on S–N curves developed from tests of component-type welded specimens. BS 7608 [22], published by the British Standards Institution, is a comprehensive weldment design code that has incorporated fatigue provisions of standards for highway and railway bridges, cranes, and offshore structures. It is applicable to many fields of engineering and provides eight classes of S–N design curves for many different steel weldments. The classes are B, C, D, E, F, F2, G, and W, and typical descriptions and class examples are given in Table 12.2. Quantitative S–N design curves for variable amplitude loading are given in Fig. 12.10. These eight S–N curves are recommended for fatigue design of most steel weldments. They are based upon many fatigue tests involving many different weldment configurations and a wide variety of steels, ultimate tensile strengths, and mean stresses. Based upon the small influence of ultimate strength and mean stress, as discussed in Section 12.2, the fatigue design S–N curves shown in Fig. 12.10 are independent of S_u and S_m. The S–N curve for a given class, B to W, is applicable to many different weldment configurations and is based on mean S–N data or mean minus 1 (mean − 1SD) or two standard deviations (mean − 2SD). The classes do not relate to weldment quality, but more to fatigue cracking locations. The curves of Fig. 12.10 are based upon recommended usage of mean fatigue behavior (50 percent survival) minus two standard deviations (mean − 2SD). Assuming a log-normal distribution on life, this results in a calculated survival of over 97 percent with a confidence level of 50 percent.

The S–N curves for each of the eight classes shown in Fig. 12.10 are modeled as log-log straight lines, analogous to Basquin's equation. However, the inverse slope, m, as defined in Fig. 12.10 is used along with the nominal stress range near the weld detail, ΔS, not S_a. For fatigue life $N_f \leq 10^7$ cycles the S–N equation for a given class is

$$N_f\,(\Delta S)^m = C \quad \text{for } N_f \leq 10^7 \text{ cycles} \tag{12.1}$$

where $m = 3$, 3.5, or 4 according to the class. C is obtained from the fatigue strength at 10^7 cycles. Values of m and C for $N_f \leq 10^7$ cycles are given in Table 12.2 in SI units for each class for both mean and (mean − 2SD) curves. Note that BS 7608 uses the coefficient C as C_0, C_1, and C_2 for mean (mean − 1SD), and (mean − 2SD) S–N curves, respectively. We shall use C as a generic coefficient but recognizing that the value of C depends upon the chosen probability of survival. The equations can be extrapolated to higher fatigue strengths until S_{max} reaches a static design criterion such as yield strength or ultimate strength. For constant amplitude loading, a fatigue limit is assumed at 10^7 cycles and the curves become horizontal (not shown in Fig. 12.10). However, for variable amplitude loading, a continued decrease in fatigue resistance is assumed for $N_f \geq 10^7$ cycles. The inverse slope for this region is taken as $m + 2$, as shown in Fig. 12.10, i.e., 5, 5.5, and 6, resulting in the equation

$$N_f\,(\Delta S)^{m+2} = C \quad \text{for } N_f \geq 10^7 \text{ cycles} \tag{12.2}$$

The coefficients C for $N_f \geq 10^7$ cycles will be different than C for $N_f \leq 10^7$ cycles. A thickness correction is also recommended, since weldment fatigue resistance has been found to decrease with an increase in plate thickness. The right side of Eqs. 12.1 and 12.2 are multiplied by the thickness correction, which for nontubular welded joints is

$$(22/t)^{0.25} \tag{12.3}$$

where the plate thickness, t, is in mm. If $t < 22$ mm, no correction is made.

Values of ΔS at 10^7 cycles are given in Table 12.2 as $2S_f$ for the eight different classes. Since the S–N curves are independent of mean stress, the values at 10^7 cycles can represent fully reversed, $R = -1$, constant amplitude fatigue limit ranges. Values of $2S_f$ or S_f can then be compared within the classes or with other notched components. The extremes of ΔS at 10^7 cycles, i.e., $2S_f$, for the recommended (mean − 2SD) curves, are 100 MPa (14.5 ksi) for class B and 25 MPa (3.6 ksi) for class W. This represents a 4 to 1 difference in weldment fatigue strength. At $\Delta S = 50$ MPa (7.25 ksi), a difference in fatigue life of two orders of magnitude occurs, and at $\Delta S = 100$ MPa (14.5 ksi) a 70 to 1 ratio in fatigue life exists for the recommended (mean − 2SD) curves. Thus, based on fatigue strength or fatigue life, a significant difference in fatigue resistance exists in these eight steel weldment classes. The recommended (mean − 2SD) fatigue strength extremes, $2S_f$, at 10^7 cycles yield values of S_f between 50 MPa (7.2 ksi) and 12.5 MPa (1.8 ksi). These values are only a fraction of the ultimate tensile strengths and have values similar to S_{CAT} from Section 7.2.3 and to threshold stress ranges obtained from region I ΔK_{th} values, similar to Fig. 6.16. This indicates that S_f for

TABLE 12.2 BS 7608 Standard Weldment Classes, Selected Examples of Each Class, and Fatigue Design Curve Values: Units for MPa and Cycles [4,22]

Class	Description and Class Example (Arrows Indicate Direction of Loading)		Curve	$N_f \leq 10^7$ m	C	$N_f = 10^7$ $2S_f$ MPa
B	Butt weld with penetration and no backing strip. Weld reinforcement dressed flush.	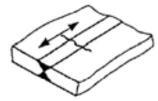	Mean	4.0	2.34×10^{15}	124
			Mean − 2SD		1.01×10^{15}	100
C	Fillet and butt welded joints made from one or both sides. Automatic weld with no stop/starts.	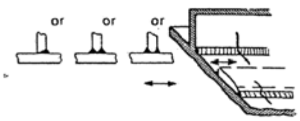	Mean	3.5	1.08×10^{14}	102
			Mean − 2SD		4.22×10^{13}	78
D	Transverse butt weld joining two single plates together. Overfill profile $\mu > 150°$.	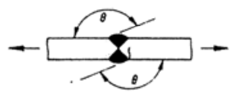	Mean	3.0	3.99×10^{12}	74
			Mean − 2SD		1.52×10^{12}	53
E	Intermittent fillet welds with g/h < 2.5.	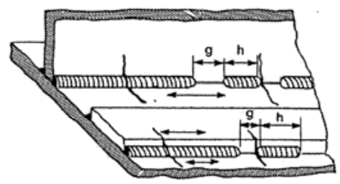	Mean	3.0	3.29×10^{12}	69
			Mean − 2SD		1.04×10^{12}	47
F	Fillet weld at cope hole, for weld continuing around plate ends or not.	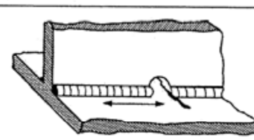	Mean	3.0	1.73×10^{12}	56
			Mean − 2SD		6.33×10^{11}	40
F_2	Partial penetration butt or fillet weld.	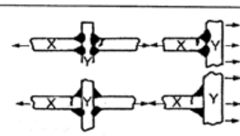	Mean	3.0	1.23×10^{12}	50
			Mean − 2SD		4.3×10^{11}	35
G	Fillet welded lap joints between plates or sections.	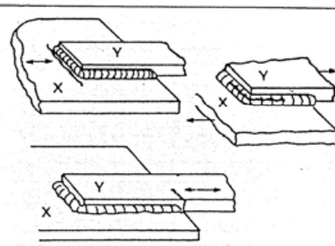	Mean	3.0	5.66×10^{11}	38
			Mean − 2SD		2.50×10^{11}	29
W	Partial penetration weld. Refers to fatigue failure across weld throat based on stress range on weld throat area.	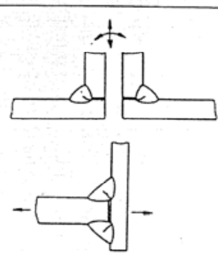	Mean	3.0	3.68×10^{11}	33
			Mean − 2SD		1.6×10^{11}	25

Reprinted with permission of the British Standards Institute.

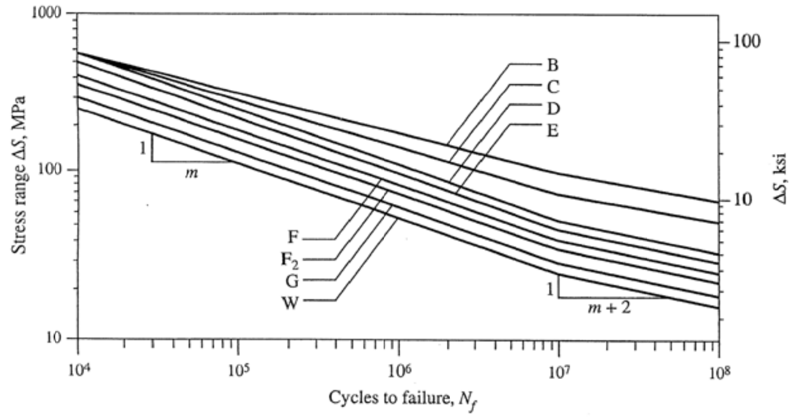

Figure 12.10 BS 7608 standard S–N weldment fatigue design curves (mean - 2SD) for variable amplitude loading of steels [22] (reprinted by permission of the British Standards Institute).

weldments is closely associated with threshold stresses for nonpropagating cracks. Fatigue design codes for aluminum alloys are also very similar to these described for steels, except that different values of C and m exist with the S–N curves. The models in Fig. 12.10 and Table 12.2 can be used in variable amplitude loading using rainflow counting and the Palmgren-Miner linear damage rule, as discussed in Chapter 9. These models can be incorporated into commercial or in-house computer fatigue software. For unprotected seawater environments, Eq. 12.1 for each weldment class is reduced by a factor of 2 on life in BS 7608 and then is linearly extrapolated to all values of N_f with a slope of m.

Example Problem Using BS 7608 A full penetration butt weld joins two 10×50 mm cross section steel plates. A constant amplitude axial load with an R ratio of -0.5 is applied to the joint. It is desired to apply 5×10^5 cycles of this load to the joint. What values of P_{max} and P_{min} can be applied to achieve this life?

From Table 12.2, the full penetration butt weld for the reinforcement (overfill) profile angle θ greater than 150° is given as class D. The weldment must be inspected to determine if this is reasonable. If it is not reasonable, we must refer to BS 7608 for the proper class. We will assume that $\theta > 150°$ and use the class D recommended (mean − 2SD) S–N curve with $m = 3.0$ and $C = 1.52 \times 10^{12}$. From Eq. 12.1, which is independent of mean stress,

$$\Delta S = (C/N_f)^{1/m} = (1.52 \times 10^{12}/5 \times 10^5)^{1/3} = 145 \text{ MPa}$$

This value can also be obtained from Fig. 12.10 for the class D curve. For $R = -0.5$

$$P_{min} = -0.5P_{max}$$

$$\Delta S = \Delta P/A = (P_{max} - P_{min})/A = (P_{max} + 0.5P_{max})/A$$
$$= 1.5P_{max}/(50)(10) = 145 \text{ MPa}$$

resulting in

$$P_{max} = \underline{48 \text{ kN}} \quad \text{and then} \quad P_{min} = \underline{-24 \text{ kN}}$$

Thus, according to the BS 7608 recommended procedure, a force varying from −24 to 48 kN could be applied to this axial loaded butt welded joint without a fatigue failure in 5×10^5 cycles.

Hot-Spot Stress/Strain Range The nominal value of ΔS near the weld detail in Eqs. 12.1 and 12.2 may be difficult to obtain in complex weldments, and/or a particular class of weldments may be difficult to ascertain. To circumvent these complexities, a "hot-spot stress range" has been defined to use with a special class T S–N curve similar to class D for all weldments [22]. The hot-spot stress range is computed or measured adjacent to and perpendicular to the weld toe. It is a linear extrapolation of the maximum nominal principal stress in the weld vicinity to the weld toe. It does not incorporate the weld geometrical stress concentration at the toe, since this is already incorporated into the recommended empirical S–N design curve. A hot-spot strain range can be measured adjacent to the weld toe. This measurement should be taken after stable hysteresis loops are formed. These hot-spot stress or strain ranges can be used under constant amplitude loading or with variable amplitude loading by using rainflow cycle counting and the Palmgren-Miner linear damage model. Additional information on use of the hot-spot stress or hot-spot strain range can be found in [16,20,22].

Fitness-for-Purpose Initial planar or volumetric discontinuities in weldments discussed in Section 12.1 play a key role in weldment fatigue design. Nondestructive inspection (NDI) can provide quantitative information on their size and location. These discontinuities may or may not be acceptable for a given service. This acceptance determination for planar (crack-like) discontinuities involves fracture mechanics concepts presented in Chapter 6 that are incorporated within a fitness-for-purpose design philosophy established by the welding profession. This could also be called "fitness-for-service." The British Standards Institution guide PD 6493 [24] provides significant guidelines for evaluating discontinuity acceptability in weldments including fracture, plastic collapse, and fatigue crack growth. Acceptable or unacceptable fatigue crack growth life is determined by integrating the sigmoidal

da/dN–ΔK curve from the initial crack size to the final crack size using realistic service spectra. The Paris fatigue crack growth equation can also be used. For most ferritic steels, PD 6493 uses a Paris equation based on results by Maddox [10], as given in Fig. 12.8. This equation with units of mm/cycle for da/dN and MPa$\sqrt{\text{mm}}$ for ΔK is

$$da/dN = 3 \times 10^{-13} (\Delta K)^3 \tag{12.4}$$

and for threshold behavior, the equations are

$$\Delta K_{\text{th}} = 170 - 214R \text{ MPa}\sqrt{\text{mm}} \quad \text{for } 0 \le R \le 0.5 \tag{12.5a}$$

or

$$\Delta K_{\text{th}} = 63 \text{ MPa}\sqrt{\text{mm}} \quad \text{for } R > 0.5 \tag{12.5b}$$

or

$$\Delta K_{\text{th}} = 170 \text{ MPa}\sqrt{\text{mm}} \quad \text{for } R < 0 \tag{12.5c}$$

where R is the stress ratio based on the combined applied and residual stresses. The integration results, along with a safety factor, can be used for acceptance, rejection, or repair of a specific weldment planar defect. This can also be used to establish NDI inspection periods. For unprotected seawater conditions, Eq. 12.4 is taken as

$$da/dN = 2.3 \times 10^{-12} (\Delta K)^3 \tag{12.6}$$

where again, da/dN is in mm/cycle and ΔK is in MPa$\sqrt{\text{mm}}$. Equations 12.5 a–c remain unchanged. For nonferrous metals with Young's modulus, E, PD 6493 uses

$$da/dN = 3 \times 10^{-13} (\Delta K)^3 (E_{\text{steel}}/E)^3 \tag{12.7}$$

with units of mm/cycle for da/dN and MPa$\sqrt{\text{mm}}$ for ΔK and

$$\Delta K_{\text{th}} = \Delta K_{\text{th,steel}}(E/E_{\text{steel}}) \tag{12.8}$$

For volumetric discontinuities (porosity or slag inclusions) PD 6493 uses S–N curve comparisons relating to different levels of porosity or inclusion severity. This provides an acceptance, rejection, or repair criterion.

Additional sources of information on the many aspects of weldment fatigue design are [25–31].

12.5 SUMMARY

Lower-strength steels and aluminum alloys are the most common metals welded. The fatigue resistance of these weldments is rather independent of the base metal's ultimate tensile strength and applied mean stress. However, weldment fatigue life is strongly dependent upon applied stress range, ΔS, weld geometry, and the size and distribution of microscopic and macroscopic discontinuities. The geometry and other discontinuities are influenced by welding procedures. The discontinuities can be planar, such as shrinkage cracks and partial penetration; volumetric, such as porosity and slag inclusions; or geometric, such as weld toe radius, undercutting, and misalignment. Fatigue cracks nucleate and/or grow from these discontinuities, usually at the weld toe or weld root, and can grow in the base metal, weld metal, and/or heat-affected zone. The material fatigue properties of these three regions are often similar. Residual stresses can also be important in weldment fatigue behavior and are usually tensile in the weld region after welding. They can be as high as the yield strength. However, since many weldments are of lower strength, relaxation of residual stresses under service loading is common. This is beneficial for relaxing undesirable welding tensile residual stresses, but it is undesirable for relaxing deliberate post weld compressive residual stresses induced by shot-peening or other methods. Careful control of shot-peening has provided significant improvements in weldment fatigue resistance. Overload stressing for one-direction loading has also been very beneficial. Thermal stress relief has provided some improvements in long-life fatigue resistance, along with little effect if tensile loads dominate. Reducing the geometric stress concentration of weldments by methods such as carefully grinding off the weld reinforcement in butt welds and carefully grinding the toes of fillet welds or using TIG dressing at weld toes may significantly improve fatigue resistance.

Weldment fatigue design can, and has, involved S–N, ε–N, da/dN–ΔK, and the two-stage methods. However, weldments present additional fatigue complexities in comparison to other components since each specific weldment contains different macro and micro discontinuities and residual stresses. Discontinuities may be crack-like; hence, fatigue life is entirely fatigue crack growth. Or they may be negligible or more rounded, providing both fatigue crack nucleation and fatigue crack growth lives. To circumvent these weldment complexities, national and international design codes have been established based upon enormous weldment test programs conducted over many years. These weldment design codes are primarily based on S–N methods and to a lesser extent on da/dN–ΔK methods. Fatigue strength design amplitudes at 10^7 cycles from BS 7608 for steels vary from 12.5 to 50 MPa (~2 to 7 ksi), which is a very small percentage of the ultimate tensile strength of the base metal. These values are consistent with threshold stress amplitudes for non-propagating cracks.

To overcome the difficulty of determining nominal applied stress ranges and weldment classes, a hot-spot stress or hot-spot strain range has been incorporated into some design codes for use with a single specific S–N curve. Fitness-for-purpose is a key methodology for determining if a specific defect can be accepted, rejected, or repaired. Service inspection periods using NDI can also be established using fitness-for-purpose procedures.

12.6 DOS AND DON'TS IN DESIGN

1. Do recognize that S–N, ε-N, da/dN–ΔK, and the two-stage methods outlined in previous chapters for constant and variable amplitude loading can be applied to weldments.
2. Do refer to the many weldment fatigue design codes available.
3. Do recognize that weldment fatigue resistance is less dependent on ultimate tensile strength of the base metal and mean stress and more dependent on applied stress range and class of weld.
4. Do reduce stress concentrations by grinding (significant care is needed) butt welds flush and smooth, dressing fillet welds, and avoiding undercuts and stray arc strikes.
5. Don't locate joints in regions of high tensile stress, and do avoid large variations in stiffness.
6. Don't use intermittent welds, and use butt welds rather than fillet welds.
7. Do consider methods such as shot- or hammer-peening, surface rolling, tensile overloading, and local heating to induce desirable surface compressive residual stresses. Careful control is needed.

REFERENCES

1. K. G. Richards, "Fatigue Strength of Welded Structures," The Welding Institute, Cambridge, May 1969.
2. P. Albrecht, "A Study of Fatigue Striations in Weld Toe Cracks," *Fatigue Testing of Weldments,* D. W. Hoeppner, ed., ASTM STP 648, ASTM, West Conshohocken, PA, 1978, p. 197.
3. T. Jutla, "Fatigue and Fracture Control of Weldments," *Fatigue and Fracture, ASM Handbook,* Vol. 19, ASM International, Materials Park, OH, 1996, p. 434.
4. S. J. Maddox, *Fatigue Strength of Welded Structures,* 2nd ed., Abington Publishing, Cambridge, England, 1991.
5. R. C. Rice, ed., *SAE Fatigue Design Handbook,* AE-22, 3rd ed., SAE, Warrendale, PA, 1997.
6. F. V. Lawrence, S. D. Dimitrakis, and W. H. Munse, "Factors Influencing Weldment Fatigue," *Fatigue and Fracture, ASM Handbook,* Vol. 19, ASM International, Materials Park, OH, 1996, p. 274.

7. H. S. Reemsnyder, "Development and Application of Fatigue Data for Structural Steel Weldments," *Fatigue Testing of Weldments,* D. W. Hoeppner, ed., ASTM STP 648, ASTM, West Conshohocken, PA, 1978, p. 3.
8. W. W. Sanders, Jr., and F. V. Lawrence, Jr., "Fatigue Behavior of Aluminum Alloy Weldments," *Fatigue Testing of Weldments,* D. W. Hoeppner, ed., ASTM STP 648, ASTM, West Conshohocken, PA, 1978, p. 22.
9. Y. Higashida, J. D. Burk, and F. V. Lawrence, Jr., "Strain-Controlled Fatigue Behavior of ASTM A36 and A514 Grade F Steels and 5083-0 Aluminum Weld Materials," *Welding J.,* Vol. 57, 1978, p. 334s.
10. S. J. Maddox, "Assessing the Significance of Flaws in Welds Subject to Fatigue," *Welding J.,* Vol. 53, 1974, p. 401s.
11. L. A. James, "Fatigue-Crack Propagation Behavior of Several Pressure Vessel Steels and Weldments," *Welding J.,* Vol. 56, 1977, p. 386s.
12. H. S. Reemsnyder, "Modeling of the Fatigue Resistance of Single-Lap Spot-Welded Steel Sheet," Document XIII-1469-92, International Institute of Welding, 1992. Available through the American Welding Society, Miami, FL.
13. D. Weber, "Evaluation of Possible Life Improvement Methods for Aluminum-Zinc-Magnesium Fillet-Welded Details," *Fatigue Testing of Weldments,* D. W. Hoeppner, ed., ASTM STP 648, ASTM, West Conshohocken, PA, 1978, p. 73.
14. H. Tada, P. C. Paris, and G. R. Irwin, *The Stress Analysis of Cracks Handbook,* 2nd ed., Paris Productions, St. Louis, MO, 1985.
15. Y. Murakami, ed. in chief, *Stress Intensity Factors Handbook,* Vol. 2, Pergamon Press, Oxford, 1987.
16. *Structural Welding Code—Steel,* ANSI/AWS D1.1-98, American Welding Society, Miami, FL, 1998.
17. "Specifications for Structural Steel Buildings—Allowable Stress Design, Plastic Design," AISC S335, American Institute of Steel Construction, Chicago, 1989.
18. "Guide, Specifications for Fracture Critical Non-redundant Steel Bridge Members," American Association of State Highway and Transportation Officials, Washington, DC, 1991.
19. "Fatigue Design of New Freight Cars," *Manual of Standards and Recommended Practice,* Section C, Vol. 2, Chapter 7, Association of American Railroads, Washington, DC, 1994.
20. "API Recommended Practice for Planning, Designing and Constructing Fixed Offshore Platforms—Working Stress Design," API 2A-WSD, 20th ed., American Petroleum Institution, Washington, DC, 1996.
21. *ASME Boiler and Pressure Vessel Code,* Section IX, American Society of Mechanical Engineers, New York, 1998.
22. "Code of Practice for Fatigue Design and Assessment of Steel Structures," BS 7608:1993, British Standards Institution, London, 1993.
23. "Offshore Installations: Guidance on Design Construction and Certification," 4th ed., U.K. Department of Energy, Her Majesty's Stationery Office, London, 1993.
24. "Guidance on Methods for Assessing the Acceptability of Flaws in Fusion Welded Structures," PD 6493:1991, 2nd ed., British Standards Institution, London, 1991.

25. W. H. Munse and L. Grover, *Fatigue of Welded Structures,* Welding Research Council, New York, 1964.

26. T. R. Gurney, *Fatigue of Welded Structures,* 2nd ed., Cambridge University Press, Cambridge, 1979.

27. S. J. Maddox, ed., *Proceedings of the International Conference on Fatigue of Welded Construction,* Brighton, England, The Welding Institute, Cambridge, 1987.

28. D. Radaj, *Design and Analysis of Fatigue Resistant Welded Structures,* John Wiley and Sons, New York, 1990.

29. A. Hobbacher, *Fatigue Design of Welded Joints and Components,* The International Institute of Welding, Abington Publishing, Cambridge, 1996.

30. M. L. Sharp, G. E. Nordmark, and C. C. Menzemer, *Fatigue Design of Aluminum Components and Structures,* McGraw-Hill Book Co., New York, 1996.

31. D. Radaj and C. M. Sonsino, *Fatigue Assessment of Welded Joints by Local Approaches,* Abington Publishing, Cambridge, 1998.

PROBLEMS

1. A longitudinal butt welded structural steel plate with width $w = 50$ mm and thickness $t = 8$ mm is subjected to an axial load $P_{min} = 3$ kN. What value of P_{max} do you recommend such that 10 million cycles can be applied without fracture for full penetration with weld bead excess material ground off?

2. Repeat Problem 1 if only 50 000 cycles are required.

3. A plate with width $w = 50$ mm and thickness $t = 8$ mm is welded to a wider plate as a lap joint. If P_{min} is 3 kN, what P_{max} can be applied for (*a*) 10 million cycles, and (*b*) 50 000 cycles?

4. Determine the fatigue coefficient C in Eq. 12.2 for $N_f \geq 10^7$ cycles using class F_2 weldment.

5. A partial penetration T joint is subjected to the following variable amplitude nominal stress spectrum (one block). How many blocks of this stress spectrum can be applied without fatigue failure?

n (cycles applied)	10^3	10^4	10^3	10^5
S_{max} (MPa)	50	25	100	50
S_{min} (MPa)	10	−25	50	25

6. A butt welded A36 steel plate is subjected to fully reversed bending. A small strain gage is bonded to the plate directly at the weld toe and reads a stable strain range $\Delta\varepsilon = 0.02$. Assuming strain–life fatigue concepts, determine the expected number of cycles to the appearance of a small crack. Repeat the problem if the strain gage reads $\Delta\varepsilon = 0.005$.

7. A full penetration transverse butt welded structure of steel plate with $w = 50$ mm and $t = 10$ mm was subjected to axial repeated loads. A nondestructive inspection indicated that a crack existed at the weld bead toe. It was less than 1 mm deep across the entire section. If $P_{min} = 0$, estimate the value of P_{max} that can be applied without the crack growing to fracture for 50 000 additional cycles. Use a safety factor of 2 on life. List all of your assumptions and comment on the validity of your solution.

8. What can you do to increase the life of the component in Problem 7 assuming that the operating load P_{max} found in Problem 7 cannot be reduced?